Electrospinning of Fluorescent Fibers from CdSe/ZnS Quantum Dots in Cellulose Triacetate

Tiffany Abitbol, Jordan T. Wilson, Derek G. Gray

Department of Chemistry, McGill University, Montreal, Quebec H3A 2A7, Canada

Received 5 March 2010; accepted 9 May 2010
DOI 10.1002/app.32782
Published online 27 July 2010 in Wiley Online Library (wileyonlinelibrary.com).

ABSTRACT: Fluorescent cellulose triacetate (CTA) fibers were prepared by electrospinning solutions of CTA dissolved in an 8 : 2 v/v cosolvent system of methylene chloride (MC) and methanol (MeOH) which contained CdSe/ZnS quantum dots (QDs). The relatively low loading of colloidal nanoparticles was sufficient to impart fluorescence to the fibers but did not significantly alter fiber morphologies, which tended toward smooth surfaces with the occasional longitudinal feature. The fibers were birefringent due to the alignment of the polymer chains which occurred during electrospinning and had widths on the order of a hundred nanometers. © 2010 Wiley Periodicals, Inc. J Appl Polym Sci 119: 803–810, 2011

Key words: cellulose triacetate; electrospun fibers; CdSe/ZnS quantum dots; fluorescence

INTRODUCTION

Electrospinning is an established and experimentally straightforward technique, which has the potential to produce virtually continuous lengths of submicron width fibers, from a wide range of materials, including many polymers and blends.[1–5] Electrospun fibers have been proposed for many different types of applications including filtration, textiles,[6] tissue engineering,[7–10] optical and electronic devices,[11,12] and sensing.[13,14] The properties of electrospun polymer fibers can be further enhanced by the incorporation of functional materials, such as polymer (i.e., to make a blend),[15,16] metal complexes,[17–19] nanoparticles,[12,20–23] carbon nanotubes,[24,25] dye molecules,[12] dye loaded zeolite crystals,[26] or proteins.[14,27]

In a typical experiment, a high voltage (kV) is applied to a metallic capillary through which the polymeric solution is fed. The charges induced on the surface of the pendant polymer droplet act in opposition to the surface tension of the fluid. Above a critical voltage, repulsive Coulombic interactions overcome surface tension, causing an electrified polymer jet to be accelerated from the apex of the droplet towards a grounded collector, located some fixed distance away. The polymer jet is elongated into a long, thin filament as the solvent evaporates and is deposited onto the collector in the form of fibers. Depending upon the nature of collection, fibers may be collected in random mats or in more ordered assemblies. The elongational flow of the polymer to some degree results in orientation of the macromolecular chains in the fibers and to interesting uniaxial properties such as birefringence.[2,4,28] The morphologies and dimensions of electrospun fibers are dependent upon the often complex interrelationship between intrinsic polymeric and solution properties, processing parameters, and ambient conditions.[4]

In this article, we describe the electrospinning of CTA fibers containing CdSe/ZnS quantum dots (QDs) from a mixed solvent composed of methylene chloride (MC) and methanol. The fluorescence of the fibers was derived from the colloidal QDs which were incorporated into the electrospinning solutions. The quantum confinement of excitons in semiconductor nanoparticles results in unique electronic properties.[29–31] Briefly, the energetic spacing between the valence and conduction bands increases with decreasing particle size giving rise to size dependent characteristics, which include broad excitation and sharp fluorescence. For fluorescent applications this translates into smaller nanoparticles emitting bluer wavelengths compared to larger nanoparticles and a potential for creating single systems, which incorporate QDs having discrete fluorescent wavelengths. The QDs used in this study are core-shell nanoparticles with a CdSe core and a ZnS shell. The CdSe core has a lower band-gap compared to the ZnS outer layer and largely defines the optical characteristics of the particles, whereas the ZnS shell improves the optical efficiency and stability of the particles.[32] In comparison to organic

Correspondence to: D. G. Gray (derek.gray@mcgill.ca).

fluorophores, surface passivated QDs possess comparable quantum yields but are less susceptible to photobleaching.[31]

CTA is a commercially important cellulose ester and is a key component of photographic films and liquid crystal display (LCD) screens. CTA is derived from the acetylation of cellulose and possesses a β-(1–4) glycosidic backbone with acetyl groups in place of the hydroxyl groups of cellulose.[33] Unlike native cellulose which is highly crystalline, hydrophilic, and insoluble in most solvents, cellulose triacetate is semicrystalline, hydrophobic, and readily soluble in common organic solvents, making it more amenable to solution processing. Cellulose can be regenerated by base-catalyzed de-esterification of CTA. The conversion to cellulose can be limited to the surfaces of CTA fibers and films, improving aqueous dispersibility while retaining the bulk properties of the polymeric material. In previous work,[34,35] we have shown that CTA is an appropriate polymeric matrix for CdSe/ZnS QDs and that surface hydrolysis to cellulose made the fluorescent materials water dispersible and able to adhere to other cellulose surfaces. The electrospinning conditions described in this article are similar to those used by Han et al.[36] who made CTA fibers from mixtures of ethanol and methylene chloride, and established the practicability of preparing CTA fibers using the electrospinning technique. The desirable properties of CTA, including good spinnability and compatibility with QDs, made it a highly suitable polymer for the current application. We found it relatively straightforward to prepare fluorescent CTA fibers with reasonably reproducible morphologies and dimensions from MeOH and methylene chloride mixed solvent.

A parallel electrode collector was used which resulted in the spatial alignment of fibers across the gap between electrodes.[37,38] The linear, fluorescent fibers are characterized by a high density arrangement of QDs, and the method of collection provides some degree of control over the 2D fiber architecture. The ability to produce polymeric fibers incorporating QDs and ordered arrangements of these fibers may be important for photonic and electronic devices such as polymeric lasers and light-emitting diodes.[21,30] Electrospinning seems to provide a potentially straightforward route toward the preparation of such systems.[11,20,21]

EXPERIMENTAL SECTION

Materials

Cellulose triacetate (43% acetyl content by weight, 103 kDa), and HPLC grade methanol (MeOH) and methylene chloride were purchased from Sigma-Aldrich. Commercial suspensions of trioctylphosphine oxide (TOPO) capped CdSe/ZnS quantum dots in toluene with nominal sizes of 2.1–5.2 nm and approximate quantum yields of 30–50% were obtained from Evident Technologies. All materials were used as received.

Preparation of electrospinning solutions

CTA solutions in methylene chloride and alcohol mixed solvent (65 g/L) were prepared in the following ratios: 10 and 20% v/v solutions of methanol in methylene chloride. The spinning solutions incorporating QDs were prepared from CTA dissolved in 20% by volume methanol in methylene chloride. The fluorescent solutions had a first excitation peak absorbance of $\sim$ 0.01 units, corresponding to an approximate QD loading of less than 1% by weight.

Electrospinning

A horizontal set-up was used. The voltage was fixed at 15 kV, the solution flow rate at 1 mL/h and the distance between capillary and collector at 10 cm. Depending upon the subsequent characterization, the grounded collector consisted of either a piece of metal foil or parallel metallic electrodes held in place by a plastic clamp which allowed the distance between electrodes to be adjusted. The parallel electrode collection allowed the fibers to be directly transferred onto a substrate for analysis. The experiments were repeated at least twice with fresh solutions at ambient temperature (about 20°C) and relative humidity (about 30–50%).

Scanning electron microscopy

Morphologies and fiber dimensions were determined from SEM images obtained using a Hitachi S-4700 cold field emission scanning electron microscope (FE-SEM). Prior to imaging the samples were sputter coated with Au-Pd using a Technics Hummer IV Sputter/Coater System.

Polarized optical microscopy

A Nikon Eclipse LV100POL microscope was used to observe the fibers under polarized light.

Differential scanning calorimetry

The thermal properties of the fibers were studied using a TA Instruments Q2000 DSC with a heating rate of 10°C/min and sample masses of 5–10 mg.

Fluorescence and UV-Vis spectroscopy

Fluorescence spectra were recorded on a FluoroMax-2 fluorimeter (Jobin Yvon-Spex) using 400 nm excitation. UV-Vis spectra were obtained using a Cary 300 BIO UV-Vis spectrometer (Varian). Fiber spectra were obtained by transferring fiber mats onto quartz slides.

Confocal microscopy

Fluorescent images of the fibers containing QDs were obtained using a Zeiss 510 confocal microscope. The optical configuration of the microscope was optimized for the different QD emission wavelengths. Fibers incorporating 525 nm QDs (green) were visualized using a 505–550 nm band pass filter and fibers incorporating 615 nm (red) QDs were visualized using a 560 nm long pass filter. A 405 nm laser excitation was used.

RESULTS AND DISCUSSION

Prior to preparing fluorescent fibers, the properties CTA fibers which did not contain QDs were studied in order to better asses the affects, if any, resulting from the incorporation of nanoparticles into the polymer fiber. CTA fibers were prepared from mixed solvent comprised by volume of either (1) 20% MeOH and 80% MC or (2) 10% MeOH and 90% MC. As mentioned in the introduction section, CTA fibers have been successfully electrospun by Han et al.[36] who dissolved the cellulosic in mixtures of ethanol and MC. We used MeOH as the alcohol component of our solvent since our past work[35] indicated some compatibility between QDs and this solvent mixture.

In general, the SEM observations presented in Figure 1 indicated that an increase in the volume percentage of alcohol altered the fiber morphologies from porous to nonporous. As the volatility of the solvent system decreased with added alcohol, the topology of the fibers tended to smoother surfaces. The use of volatile solvents, such as MC, has been shown to produce porous fibers.[36,39,40] Replacing methylene chloride (boiling point = 40°C) with lower vapor pressure alcohols will reduce the tendency to pore formation but at the 10% by volume methanol content [Fig. 1(a)] porous morphologies were still apparent. The fibers prepared from 10% by volume MeOH solvent had widths ranging from $\sim$ 300 nm to $\sim$ 3 μm, whereas the widths of the fibers electrospun from the higher MeOH content solvent had a narrower range of $\sim$ 400 to $\sim$ 700 nm. The relatively large thicknesses are not uncommon for fibers electrospun from cellulose derivatives[28,36,41–43] and may perhaps be related to the relative stiffness of cellulosic chains. In addition,

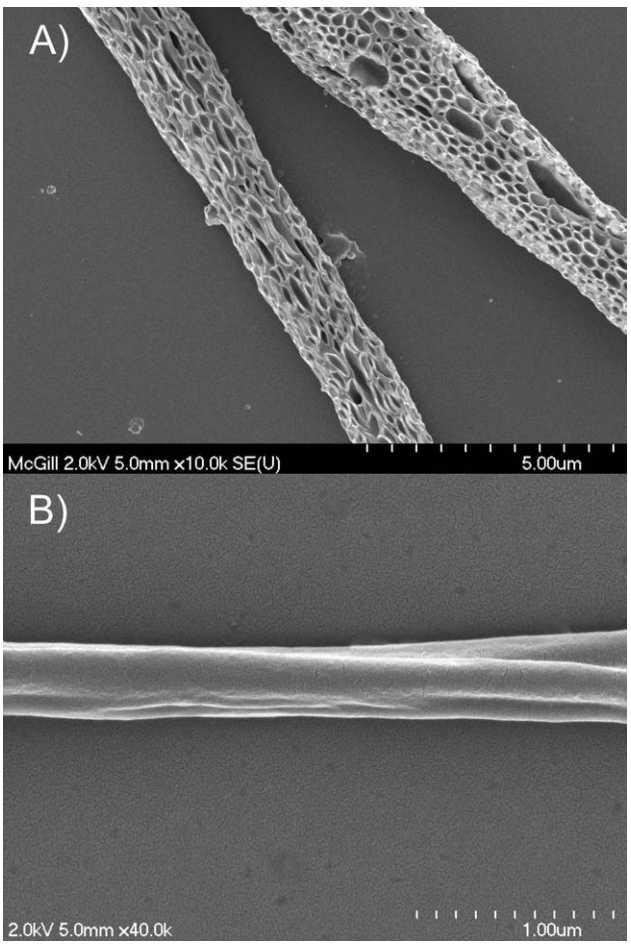

Figure 1 SEM of CTA fibers electrospun from MC and MeOH mixed solvent: (A) 10% MeOH by volume and (B) 20% MeOH by volume.

dimensions were not entirely consistent across single fibers.

The porous fibers were characterized by longitudinal pores having $\sim$ 100 nm long-axis widths, with some of the larger pores seemingly formed from coalescence of smaller ones, and by smaller pores with cross sections approaching circular. Pore formation in electrospinning is generally attributed to phase separation induced by rapid solvent evaporation.[39] For polymer solutions exhibiting an upper critical solution temperature (UCST), such as CTA, the sudden cooling caused by rapid solvent evaporation may be sufficient to quench the system into the biphasic regions of the phase diagram.[44,45] The solvent rich phase evaporates to form pores and the concentrated phase solidifies into the fiber. The dominant mechanism for the formation of pore structures in electrospun fibers, particularly when interconnected pores are observed, is generally considered to be phase separation by spinodal decomposition.[39] The rapid rates of fiber formation and solvent evaporation, characteristic of electrospinning from volatile solvent, are compatible with the fast

quench needed to bring the system into the unstable spinodal region of the phase diagram.[25] Porous structures have also been attributed to vapor induced phase separation,[45,46] the effects of humidity[40,45,46] and solvent evaporation through a polymer skin.[40] In the current system, where highly volatile methylene chloride was used under relatively high-ambient humidity and where polymer skins were formed, it is difficult to conclusively pinpoint a single pore forming process.

The fibers spun from the higher alcohol solvent compositions [Fig. 1(b)] were smooth, with longitudinal ridges. This type of feature has been previously observed by Han et al.[36] for electrospinning CTA ethanol and methylene chloride cosolvents and by Park et al.[47] who prepared ethyl cellulose fibers by electrospinning from mixtures of DMAc and THF. The corrugations, particularly when they extended in a linear fashion along the fiber lengths or disengaged from the main fiber axis, seem to indicate fiber bundles. A bundled morphology typically indicates that the fibers are still wet when they hit the collector, causing individual fibers to stick together.[48] The addition of alcohol, from 10% to 20% by volume of MeOH, decreased the overall volatility of the system and, with the electrospinning conditions used in the current experiments (i.e., 10 cm between capillary and collector), resulted in wetter fibers.

Polarized microscope images of the CTA fibers are presented in Figure 2. Due to the nature of collection, the fibers were more or less aligned with the direction of alignment indicated with arrows. Samples which are oriented or crystalline appear bright when viewed between crossed polarizers, and conversely, amorphous materials appear dark. All the electrospinning conditions resulted in fibers which appeared bright between crossed polarizers, indicating birefringence and polymer chain orientation within the fibers. Birefringent wet spun CTA fibers were prepared by Bheda et al.[42], but in that case the initial polymer solution was an ordered liquid crystalline phase. Han et al.[36] did not address the birefringence of the CTA fibers which they prepared. The observation of birefringence does not seem altogether surprising for fibers prepared from semicrystalline polymer in a mesogenic solvent, subjected to the strong elongational forces characteristic to electrospinning.

QDs were incorporated into the fibers electrospun from the higher alcohol content solvent mixture because the fibers prepared from this condition were most uniform. QDs have been previously incorporated into polymeric electrospun fibers: PLLA ands PS fibers embedded with ZnSe quantum dots were prepared by Schlecht et al.[11], PMMA fibers embedded with CdSe/ZnS quantum dots were electrospun

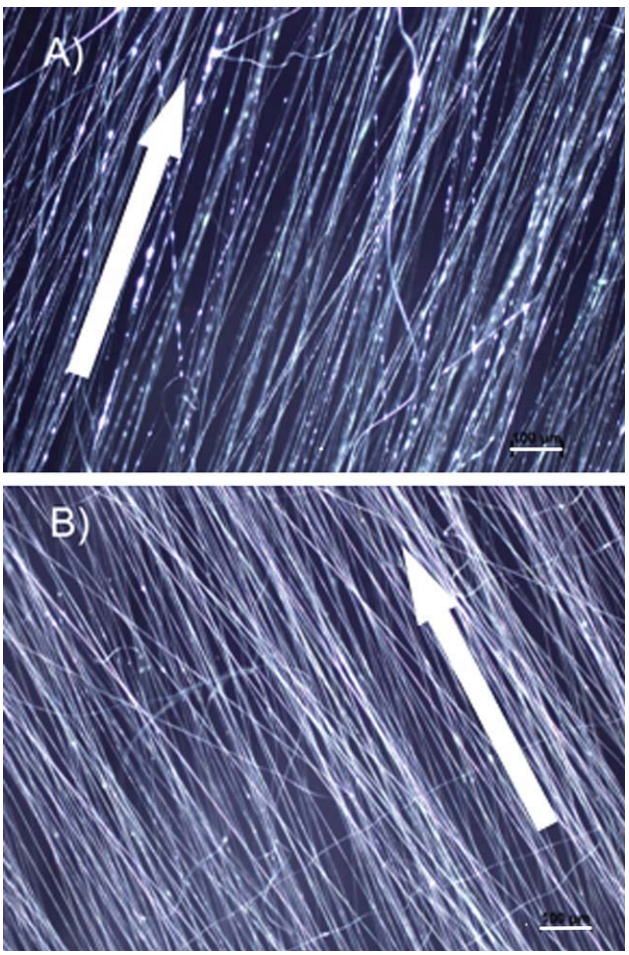

Figure 2 Polarized microscopy of CTA fibers electrospun from MC and MeOH mixed solvent: (A) 10% MeOH by volume and (B) 20% MeOH by volume. Arrows indicate direction of fiber alignment. [Color figure can be viewed in the online issue, which is available at wileyonlinelibrary.com.]

by Tomczak et al.[12] and Liu et al.[21] Spun fibers from mixtures of CdSe/ZnS QDs and light guiding polymer, Wang et al.[22] prepared fibers from cadmium acetate and polyethylene oxide (PEO) solution and treated the resultant fibers with H_2S to generate CdS nanoparticles *in-situ* and most recently Li et al.[20] made nanotubes by electrospinning mixtures of colloidal ZnO and polyvinylpyrrolidone (PVP) solution. In the current approach, small volumes ($\sim$ 0.1 mL) of CdSe/ZnS QDs in toluene (either single particle sizes or a mixture) were added to the CTA solution and fibers were obtained by electrospinning the mixture. The fluorescence and absorbance spectra of the QDs and a photograph of the spinning solutions taken under UV-illumination are presented in Figures 3 and 4, respectively.

In Figure 5, SEM images are presented of two representative fluorescent samples. The morphologies and dimensions of the fibers were found to be generally unaffected by the relatively small addition of

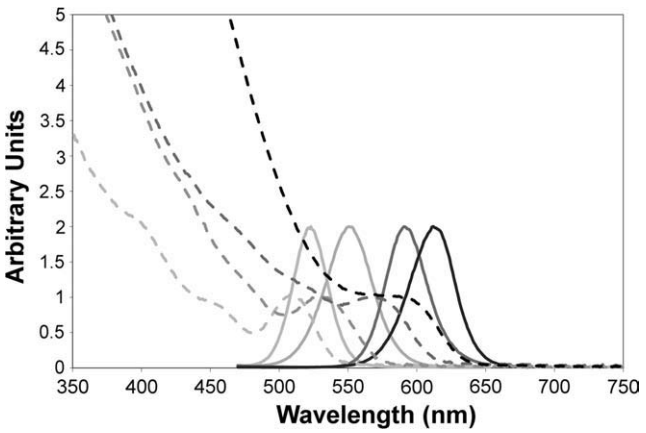

Figure 3 Absorbance (dotted lines) and fluorescence (solid lines) of QDs used in electrospinning experiments. (From left to right, increasing QD size series in toluene).

QDs, and there did not seem to be any measurable correlation between the size of the QDs and the size of the fibers. The widths of the fibers ranged from 100 nm to 2 μm.

The fluorescence of the fibers was visualized using UV-illumination (Fig. 6), fluorescence spectroscopy (Fig. 7) and confocal microscopy (Fig. 8). Figure 6 illustrates the macroscopic fluorescence of a mat of unaligned fluorescent fibers collected on a sheet of foil and Figure 7 looks at that same mat using fluorescence spectroscopy. The peak wavelength was found to be 611 nm, slightly blue-shifted compared to the fluorescence of the initial colloidal QDs. The shift to higher energy emissions has been previously observed in CTA films embedded with commercial CdSe/ZnS QDs and may be reflective of improved surface passivation of the nanoparticles.[35] Figure 8 shows confocal microscopy of the fibers, which allowed direct visualization of the fluorescence of single fibers. The fibers in Figure 8(a) contained QDs

Figure 4 Fluorescent electrospinning solutions containing QDs with fluorescence peaks at (A) 525 nm QDs, (B) 550 nm, (C) 590 nm, (D) 615 nm and (E) 525 and 615 nm. [Color figure can be viewed in the online issue, which is available at wileyonlinelibrary.com.]

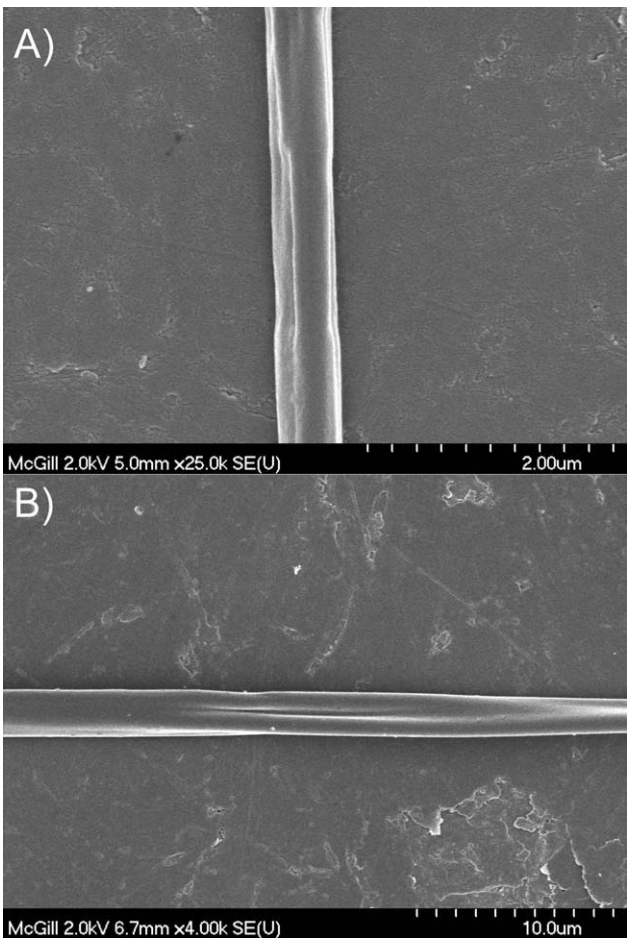

Figure 5 SEM of CTA fibers containing quantum dots with fluorescence peaks at (A) 550 nm and (B) 590 nm.

with 525 nm peak fluorescence and in Figure 8(b) two types of fibers, containing QDs which fluoresced at either 525 or 615 nm were collected onto a single substrate.

Polarized microscopy images of CTA fibers which contain QDs are shown in Figure 9. The fibers are birefringent and the addition of QDs does not seem to significantly alter the ordering of polymer chains which occurs during the electrospinning process.

Differential scanning calorimetry (DSC) was used to probe the thermal signature of the electrospun fibers, and to determine if crystalline order played a role in the observed birefringence. In Figure 10, the DSC curves for first heating are presented for commercial CTA melt-processed pellets, CTA fibers electrospun from 20% by volume alcohol content and a CTA film cast from the same solvent mixture. The thermograms for fibers containing QDs are not shown since they were very similar to those of the blank CTA fibers. The endothermic hump observed between 50 and 100°C in the CTA fiber and film thermograms is attributed to the evaporation of solvent.[49] The thermal properties of CTA have been studied extensively, and the absence of a

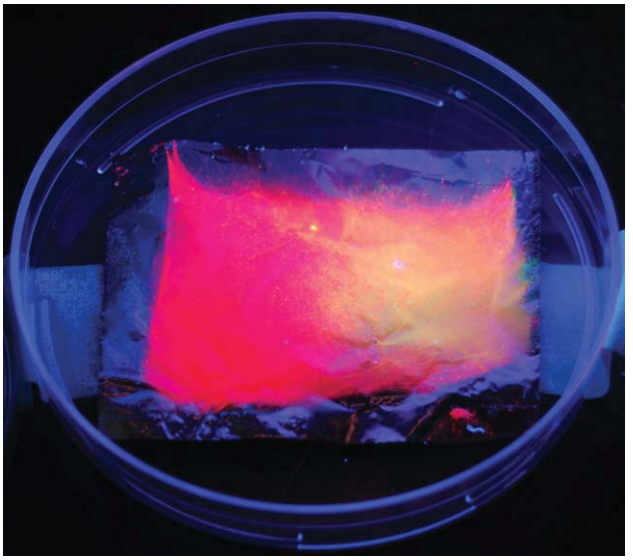

Figure 6 Macroscopic fluorescence of a mat of CTA fibers containing QDs with fluorescence at 615 nm. [Color figure can be viewed in the online issue, which is available at wileyonlinelibrary.com.]

crystallization temperature (T_c) and of a well-defined glass transition (T_g) in the commercial sample is typical.[49] In contrast, the film and fiber samples exhibited glass transition regions at $\sim$ 190°C and exothermic peaks at around 218°C, indicative of some crystallization upon heating. All samples finally melted at around 290°C. The transition of amorphous regions to crystalline domains, observed upon heating the film and fiber samples, is related to the processing of the samples. For the CTA film, the slow timescale of evaporation (about 24 h) may have allowed the chains to achieve some degree of orientation before being frozen into the film structure. The electrospun fibers were subjected to extremely rapid solvent evaporation, but also to strong stretching forces that may be sufficient to produce significant polymer chain alignment. The chain alignment induced during processing likely facilitates the crystalline transition observed upon heating.

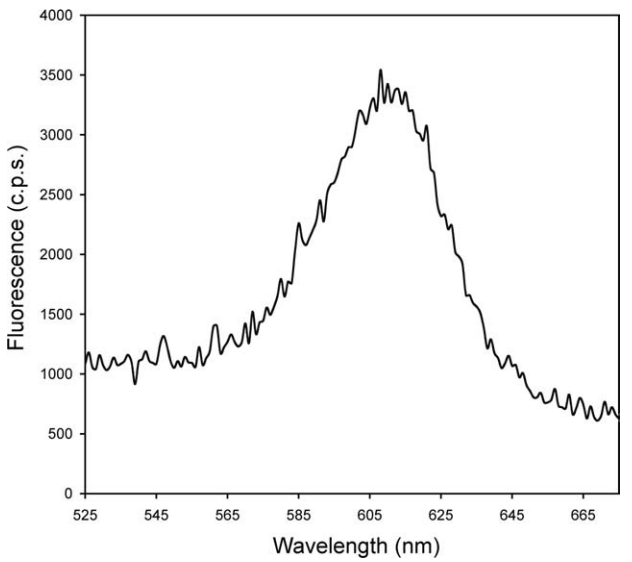

Figure 7 Fluorescence of CTA fiber mat containing QDs.

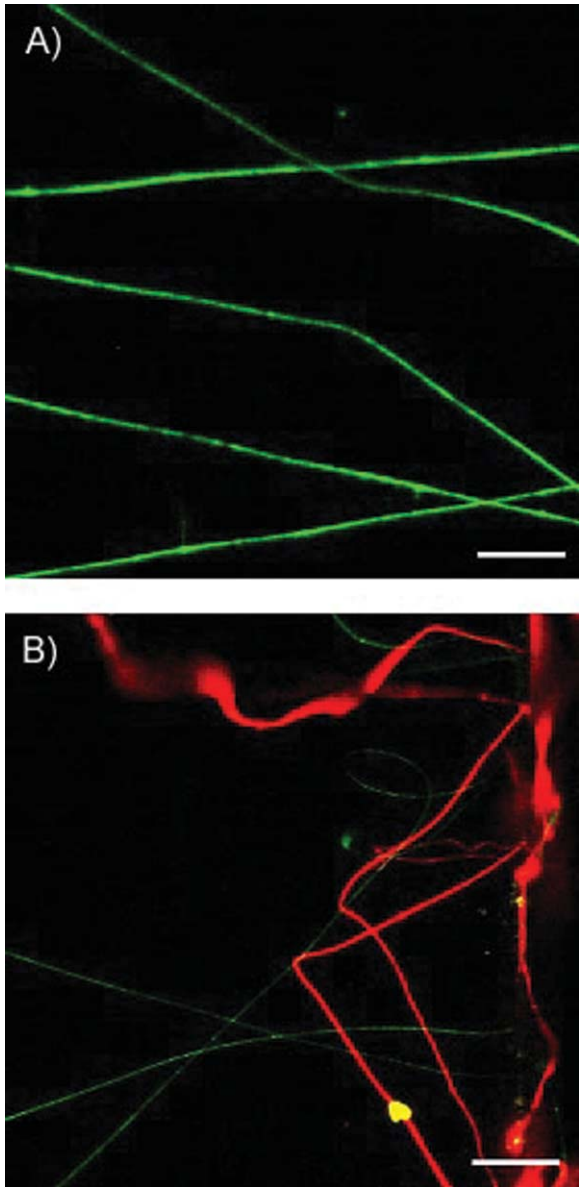

Figure 8 Confocal microscopy of fluorescent fibers: (A) fibers containing QDs with 525 nm fluorescence and (B) fibers containing QDs with either 525 or 615 nm fluorescence. (Scale bars = 20 mm). [Color figure can be viewed in the online issue, which is available at wileyonlinelibrary.com.]

The DSC data can be used to determine the degree of crystallinity by evaluating the heats of fusion of the samples (ΔH_M) and comparing those values to the heat of fusion for a 100% crystalline CTA sample (ΔH_M°). In these calculations the heat of fusion of 100% crystalline CTA was taken to be 58.8 J/g.[50] The data is summarized in Table I. The percent

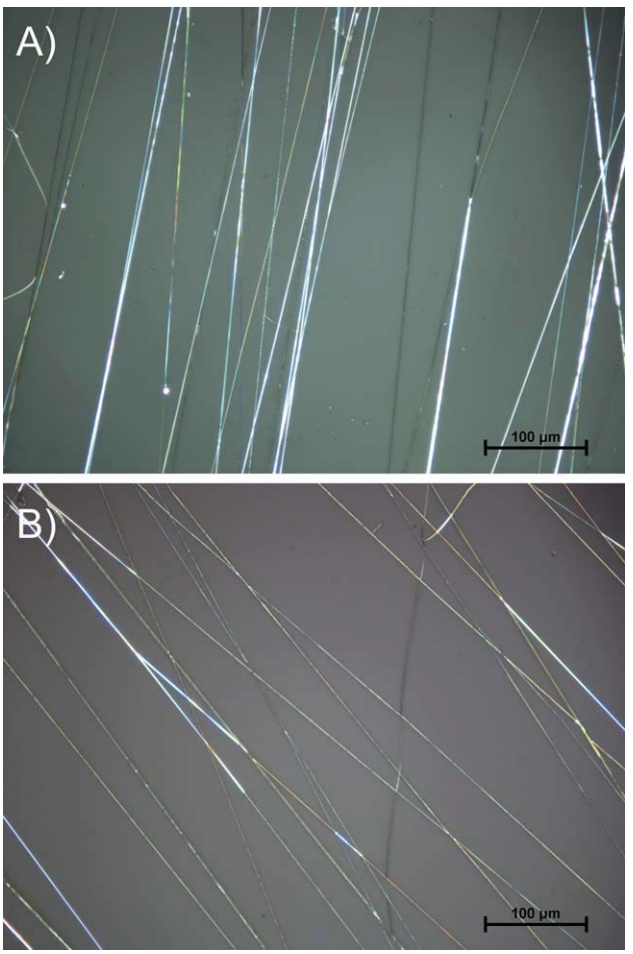

Figure 9 Polarized optical microscopy of CTA fibers containing quantum dots with fluorescence peaks at (A) 525 nm and (B) 615 nm. [Color figure can be viewed in the online issue, which is available at wileyonlinelibrary.com.]

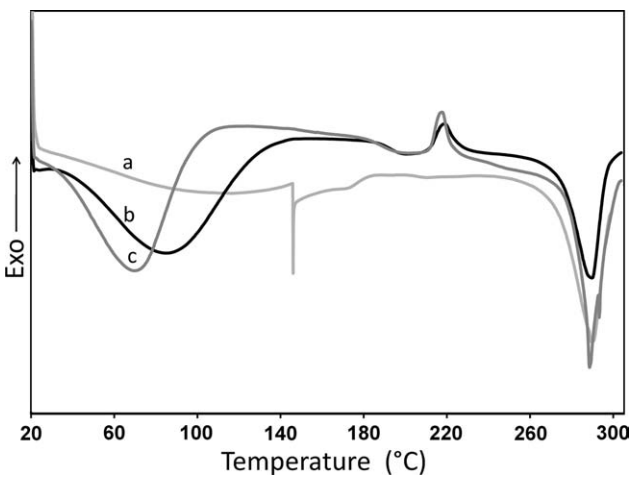

Figure 10 DSC thermograms of commercial CTA pellets, CTA film, and electrospun fibers from 8 : 2 v/v MC : MeOH solvent.

TABLE I
DSC Data for CTA Film, Fiber, and Commercial Pellets

	Tc (°C)	*Tm* (°C)	ΔH_C (J/g)	ΔH_M (J/g)	*C* (%)[a]
Pellets	n/a	289.4	0	15.2	25.8
Film	218.9	289.8	3.5	19.2	26.6
Fiber	217.7	288.6	3.2	19.8	28.2

[a] $C\ (\%) = (\Delta H_M - \Delta H_C)/\Delta H_M^{\circ}$

crystallinity of all three samples was quite similar (26–28 %) but was greatest for the fiber sample and least for the commercial pellets.

CONCLUSIONS

CTA fibers of micron and submicron widths were successfully electrospun from CTA dissolved in mixtures of methanol and methylene chloride. The fibers were macroscopically aligned by the use of a parallel electrode collector. By varying the alcohol component of the solvent it was possible to obtain fibers with either porous morphologies (lower alcohol content) or smoother morphologies (higher alcohol content). Fluorescent fibers were prepared by incorporating QDs into the CTA spinning solution and the fibers possessed morphologies similar to fibers spun from the initial polymer solution. The fibers were all found to be birefringent due to the alignment of the polymer chains which occurs during the electrospinning process.

We thank NSERC Canada and FPInnovations/Paprican for financial support, and the Centre for Self-Assembled Chemical Structures (CSACS) and Dr. S.J. Manley for use of laboratory equipment. T.A. thanks Petr Fuirasek, Dr. L. Mongeon, Dr. J. Presley, and Fred Klug for assistance with DSC, SEM, confocal microscopy, and collector fabrication, respectively, and J.M. Berry for useful discussions.

References

1. Doshi, J.; Reneker, D. H. J Electrostatics 1995, 35, 151.
2. Reneker, D. H.; Chun, I. Nanotechnology 1996, 7, 216.
3. Li, D.; Xia, Y. Adv Mater 2004, 16, 1151.
4. Greiner, A.; Wendorff, J. H. Nanotechnology 2007, 46, 5670.
5. Huang, Z.-M.; Zhang, Y.-Z.; Kotaki, M.; Ramakrishna, S. Compos Sci Technol 2003, 63, 2223.
6. Wang, S.; Yang, Q.; Du, J.; Bai, J.; Li, Y. J Appl Polym Sci 2007, 103, 2382.
7. Kwon, O. H.; Lee, I. S.; Ko, Y.-G.; Meng, W.; Jung, K.-H.; Kang, I.-K.; Ito, Y. Biomed Mater 2007, 2, S52.
8. Lee, Y. H.; Lee, J. H.; An, I.-G.; Kim, C.; Lee, D. S.; Lee, Y. K.; Nam, J.-D. Biomaterials 2005, 26, 3165.
9. Traversa, E.; Mecheri, B.; Mandoli, C.; Soliman, S.; Rinaldi, A.; Licoccia, S.; Forte, G.; Pagliari, S.; Carotenuto, F.; Minieri, M.; Di Nardo, P. J Exp Nanoscience 2008, 3, 97.
10. Pham, Q. P.; Sharma, U.; Mikos, A. G. Tissue Eng 2006, 12, 1197.
11. Schlecht, S.; Tan, S.; Yosef, M.; Dersch, R.; Wendorff, J. H.; Jia, Z.; Schaper, A. Chem Mater 2005, 17, 809.

12. Tomczak, N.; Gu, S.; Han, M.; Van Hulst, N. F.; Vansco, G. J. Eur Polym J 2006, 42, 2205.
13. Li, D.; Frey, M. W.; Baeumner, A. J. J Membr Sci 2006, 279, 354.
14. Kowalczyk, T.; Nowicka, A.; Elbaum, D.; Kowalewski, T. A. Biomacromolecules 2008, 9, 2087.
15. Zhao, Q.; Huang, Z.; Wang, C.; Zhao, Q.; Sun, H.; Wang, D. Mater Lett 2007, 61, 2159.
16. Zhao, Q.; Xin, Y.; Huang, Z.; Liu, S.; Yang, C.; Li, Y. Polymer 2007, 48, 4311.
17. Yan, E.; Wang, C.; Huang, Z.; Xin, Y.; Tong, Y. Mater Sci Eng A 2007, 464, 59.
18. Zhang, H.; Song, H.; Yu, H.; Li, S.; Bai, X.; Pan, G.; Dai, Q.; Wang, T.; Li, W.; Lu, S.; Ren, X.; Zhao, H.; Kong, X. Appl Phys Lett 2007, 90, 103103.
19. Zhang, H.; Song, H.; Dong, B.; Han, L.; Pan, G.; Bai, X.; Fan, L.; Zhao, H.; Wang, F. J Phys Chem C 2008, 112, 9155.
20. Li, X. H.; Shao, C. L.; Liu, Y. C.; Chu, X. Y.; Wang, C. H.; Zhang, B. X. J Chem Phys 2008, 129, 114708/1.
21. Liu, H.; Edel, J. B.; Bellan, L. M.; Craighead, H. G. Small 2006, 2, 495.
22. Wang, C.; Yan, E.; Sun, Z.; Jiang, Z.; Tong, Y.; Xin, Y.; Huang, Z. Macromol Mater Eng 2007, 292, 949.
23. Kriha, O.; Becker, M.; Lehmann, M.; Kriha, D.; Krieglstein, J.; Yosef, M.; Schlecht, S.; Wehrspohn, J.; Wendorff, J. H.; Greiner, A. Adv Mater 2007, 19, 2483.
24. Dror, Y.; Salalha, W.; Khalfin, R. L.; Cohen, Y.; Yarin, A. L.; Zussman, E. Langmuir 2003, 19, 7012.
25. Yeo, L. Y.; Friend, J. R. J Exp Nanoscience 2006, 1, 177.
26. Cucchi, I.; Spano, F.; Giovanella, U.; Catellani, M.; Varesano, A.; Calzaferri, G.; Botta, C. Small 2007, 3, 305.
27. Buchko, C. J.; Chen, L. C.; Shen, Y.; Martin, D. C. Polymer 1999, 40, 7397.
28. Canejo, J. P.; Borges, J. P.; Godinho, M. H.; Brogueira, P.; Teixeira, P. I. C.; Terentjev, E. M. Adv Mater 2008, 20, 4821.
29. Alivisatos, A. P. J Phys Chem 1996, 100, 13226.
30. Alivisatos, A. P. Science 1996, 271, 933.
31. Murphy, C. J. Anal Chem 2002, 74, 520A.
32. Dabbousi, B. O.; Rodriguez-Viejo, J.; Mikoulec, F. V.; Heine, J. R.; Mattoussi, H.; Ober, R.; Jensen, K. F.; Bawendi, M. G. J Phys Chem B 1997, 101, 9463.
33. El Seoud, O. A.; Heinze, T. Adv Polym Sci 2005, 186, 103.
34. Abitbol, T.; Gray, D. G. Cellulose 2009, 16, 319.
35. Abitbol, T.; Gray, D. G. Chem Mater 2007, 19, 4270.
36. Han, S. O.; Son, W. K.; Youk, J. H.; Lee, T. S.; Park, W. H. Mater Lett 2005, 59, 2998.
37. Li, D.; Wang, Y.; Xia, Y. Nano Lett 2003, 3, 1167.
38. Teo, W. E.; Ramakrishna, S. Nanotechnology 2006, 17, R89.
39. Bognitzki, M.; Czado, W.; Frese, T.; Schaper, A.; Hellwig, M.; Steinhart, M.; Greiner, A.; Wendorff, J. H. Adv Mater 2001, 13, 70.
40. Medeiros, E. S.; Mattoso, L. H. C.; Offeman, R. D.; Wood, D. F.; Orts, W. J. Can J Chem 2008, 86.
41. Frey, M. W. Polym Rev 2008, 48, 378.
42. Bheda, J.; Fellers, J. F.; White, J. L. J Appl Polym Sci 1981, 26, 3955.
43. Tungprapa, S.; Puangparn, T.; Weerasombut, M.; Jangchud, I.; Fakum, P.; Semongkhol, S.; Meechaisue, C.; Supaphol, P. Cellulose 2007, 14, 563.
44. Kim, G.-M.; Lach, R.; Michler, G. H.; Chang, Y.-W. Macromol Rapid Commun 2005, 26, 728.
45. Megelski, S.; Stephens, J. S.; Chase, D. B.; Rabolt, J. F. Macromolecules 2002, 35, 8456.
46. Casper, C. L.; Stephens, J. S.; Tassi, N. G.; Chase, D. B.; Rabolt, J. F. Macromolecules 2004, 37, 573.
47. Park, J. Y.; Han, S. W.; Lee, I. H. J Ind Eng Chem 2007, 13, 10002.
48. Deitzel, J. M.; Kleinmeyer, J.; Harris, D.; Beck Tan, N. C. Polymer 2001, 42, 261.
49. Zugenmaier, P. In Cellulose Acetates: Properties and Applications; Rustemeyer, P., Ed.; Wiley-VCH, 2004; Vol. 208, p 81.
50. Cerqueira, D.; Rodrigues Filho, G.; Assunção, R. Polym Bull 2006, 56, 475.